

The performance of the High Energy Particle Detector HEPD-02 on board CSES-02 satellite: from simulation to test beam data

Francesco Maria Follega^{a,b,*} on behalf of the Limadou HEPD Collaboration

^aUniversity of Trento,

V. Sommarive 14, I-38123 Povo (Trento), Italy

^bINFN-TIFPA,

V. Sommarive 14, I-38123 Povo (Trento), Italy

E-mail: francesco.follega@unitn.it

CSES (China Seismo-Electromagnetic Satellite) is a sophisticated multi-payload space observatory aimed to the monitoring of the Van Allen Belts dynamics, the study of solar-terrestrial interactions and the extension at low energies of existing Cosmic Ray measurements. The first satellite (CSES-01) is on orbit since February 2018, hosting on board the HEPD-01 particle detector. The second (CSES-02) will be launched during the early 2024, and will carry HEPD-02, a new high energy particle detector. HEPD-02 is optimized to detect charged particles: mostly electrons (3-100 MeV) and protons (30-200 MeV), with good capabilities in the identification of heavier nuclei. The instrument is quite compact ($40.36 \times 53.00 \times 38.15 \text{ cm}^3$) and presents important upgrades with respect to its predecessor: it will be the first instrument carrying a CMOS pixel tracker in space, designed to reach a ~ 4 micron resolution; it will mount an electromagnetic calorimeter that includes six of the largest LYSO crystals ever used in space ($15 \times 5 \times 2.5 \text{ cm}^3$). The full detector has been recently integrated, with an event reconstruction software already in place. A detailed Monte Carlo (MC) simulation was developed and an extensive beam test campaign performed to validate HEPD-02 capabilities in identification and measurement of kinetic energy and arrival direction of incoming particles. In this contribution a synthetic description of the HEPD-02 detector and its main characteristics will be given. The estimation of its scientific performances on MC simulation will be reported, with a particular focus on their assessment with the different beam test acquisitions and atmospheric muon data.

38th International Cosmic Ray Conference (ICRC2023)
26 July - 3 August, 2023
Nagoya, Japan



*Speaker

1. Scientific goals of the CSES mission

The Limadou project is the Italian contribution to the China Seismo-Electromagnetic Satellite (CSES) mission. The CSES mission [1] is a joint collaboration between the China National Space Agency (CNSA) and the Italian Space Agency (ASI) aiming to build a sophisticated space observatory focused on the monitoring of the electromagnetic environment, the plasma and particle populations in the atmosphere, ionosphere and magnetosphere. The main scientific objectives of the missions are:

- clarify on the existence and nature of a correlation between seismic events and variation of fluxes of charged particles in the Van Allen Belts;
- extend the previous measurements of low energy cosmic rays spectrum for protons, electrons and light nuclei [2, 3], from few MeV to hundreds MeV;
- measure transient events such as Particle Burst, Gamma Ray Burst and impulsive solar activity (CMEs and solar flares).

On February 2018 the first satellite of the mission (CSES-01) equipped with nine instruments, among which there was Limadou High Energy Particle Detector (HEPD-01), was launched and it is now orbiting around the Earth. It is placed on a 98° Sun-synchronous circular orbit at an altitude of about 500 km. A second satellite CSES-02 will be launched during the early 2024 on a complementary orbit with respect to CSES-01, and will carry HEPD-02, a new high energy particle detector. This instrument has been recently integrated, and it is now performing an extensive test campaign for space qualification and calibration. It presents important upgrades with respect to its predecessor, extending the physics reach of the mission: a novel MAPS-based tracker (marking the first time for a pixel tracker on a space detector), an improved electromagnetic calorimeter with additional and a new trigger logic. The addition of a second observation point will increase the spatial coverage of the mission and lead to a significant enhancement in the statistics gathered during the satellites operating time.

2. The Limadou HEPD-02 detector

Limadou HEPD-02 is optimized to detect 30-200 MeV protons, 3-100 MeV electrons and identify light nuclei in a wide range of energies. As shown in figure 1 (left), HEPD-02 is composed by several sub-detectors:

- A first EJ200 trigger plane (TR1) segmented in 5 bars (0.2 cm thick) to lower the energy threshold of the detector and increase the acceptance;
- A pixel tracker made by three layers of MAPS modules with $29 \mu\text{m}$ pitch (single hit resolution of $\sim 4 \mu\text{m}$), covering a region 15 cm x 15 cm;
- A second plastic scintillator trigger plane (TR2) segmented in 4 bars (0.8 cm thick) placed perpendicularly with respect to TR1;

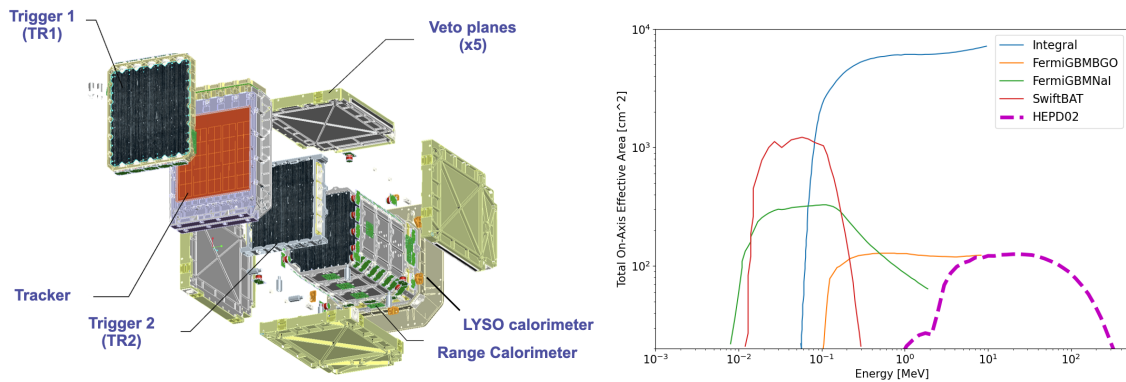


Figure 1: Exploded view of the HEPD-02 detector with all the subsystem (left) and the total effective area on axis for gamma detection (right).

- A range calorimeter made of 12 planes of plastic scintillator (150 mm x 150 mm x 10 mm), each one read out by two PMTs;
- a LYSO calorimeter mounting 6 of among the largest LYSO crystal used in space (15 cm x 5 cm x 2.5), accounting for $\sim 4.3X_0$;
- An anti-coincidence detector (Veto) made by 5 scintillator planes.

This detector and the interaction with particles have been simulated using the GEANT4 toolkit [7]. The energy deposited in the scintillator planes is converted into light, which is then collected by the PMTs in order to reproduce exactly the signal generated in our detector.

As its predecessor (HEPD-01) this detector will perform detailed measurement of charged particle flux at low energies [4, 5] and will be used to identify and monitor transient phenomena in the magnetosphere and ionosphere [6]. HEPD-02 will be able to measure Gamma Ray Burst from a few MeV to hundreds MeV, thanks to the improved LYSO calorimeter and to a dedicated trigger logic. Its total effective area (on-axis) is compared with currently operating GRB detectors in figure 1 (right).

3. HEPD-02 performance on simulated data

The simulation of HEPD-02 is structured in three consecutive layers. A first layer is represented by a truth level simulation of the interaction between the particles and the detector, realized with the GEANT4 toolkit [7]. The energy deposits, the position and the type of the interactions are recorded in all the detectors with increased precision in the sensitive materials.

Light production processes in the scintillators (LYSO crystals and EJ200 planes), as well as the propagation and the collection of photons by the PMTs are parametrized using dedicated simulations with the optical properties of the material and the Birks law [8]. This semi-parametric approach is tuned on real data acquired on ground and during the beam test campaign.

The pixel signal and the generation of the clusters produced by the energy deposits in the tracker is performed with TROPix [9]: a fast parametric tool reproducing the output of pixel detectors. This tool has been tuned on beam test data of the MAPS module used for the integration of HEPD-02.

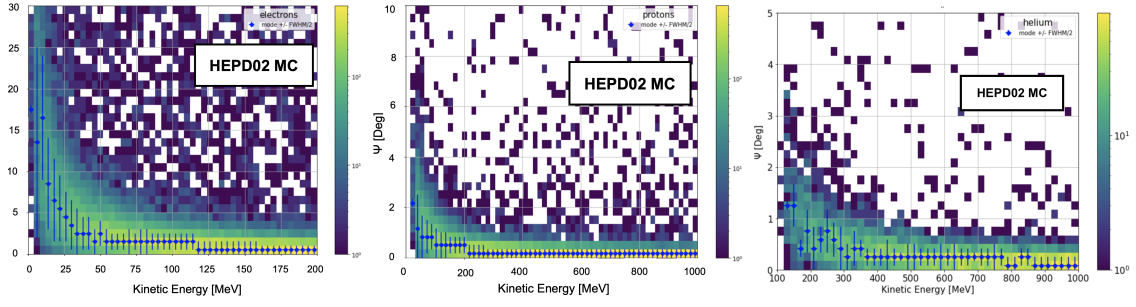


Figure 2: Angular resolution for electrons, protons and alpha particles as a function of the kinetic energy of the incoming particle. Blue points represents the mode of the projection on the y axis and the error bars the HWHM of the distribution.

The scientific performance of HEPD-02 have been evaluated with a dedicated Monte Carlo simulation for electrons, protons and alpha particles in the detection range of the apparatus. All the three layers of the simulation chain have been executed to produce a final sample containing the digitized information available in real data. Events were simulated with:

- flat energy spectrum in kinetic energy (range depending on the particle type);
- polar angle: $0^\circ < \theta < 90^\circ$, sampled uniformly in $\cos^2 \theta$ in order to guarantee an isotropic flux;
- azimuthal angle: $-180^\circ < \phi < 180^\circ$;
- particles have been generated uniformly from a $40 \times 40 \text{ cm}^2$ window (parallel to the x-y plane) right above the detector window.

Events were required to hit the first and the second trigger plane (TR1 & TR2) and therefore to leave at least two hits on the three tracker layers.

In order to reconstruct the arrival direction, several steps are performed in the event reconstruction software. Firstly, the DBSCAN [10] clustering algorithm is used to gather close-by pixel in a single object called "cluster". Then, the center-of-gravity of the cluster is calculated and used to construct track seeds with a 3D Hough transform [11]. Cluster lying close to the same track seed are used to fit a track and the angular difference between the true and reconstructed direction is computed as follow:

$$\Psi = \arccos(\vec{v}_{tr} \cdot \vec{v}_{pr}) \quad (1)$$

$$\vec{v}_{tr} = \begin{pmatrix} \sin \theta_{tr} \cos \phi_{tr} \\ \sin \theta_{tr} \sin \phi_{tr} \\ \cos \theta_{tr} \end{pmatrix}, \quad \vec{v}_{pr} = \begin{pmatrix} \sin \theta_{pr} \cos \phi_{pr} \\ \sin \theta_{pr} \sin \phi_{pr} \\ \cos \theta_{pr} \end{pmatrix}$$

The arrival direction reconstruction performance of HEPD-02 are displayed in fig 2. They show that the uncertainty of this observable is dominated by the irreducible contribution of Coulomb scattering. Therefore for low-energy electrons we have an angular resolution of $\sim 10^\circ$, while for low energy protons and helium the error is $\sim 1^\circ$.

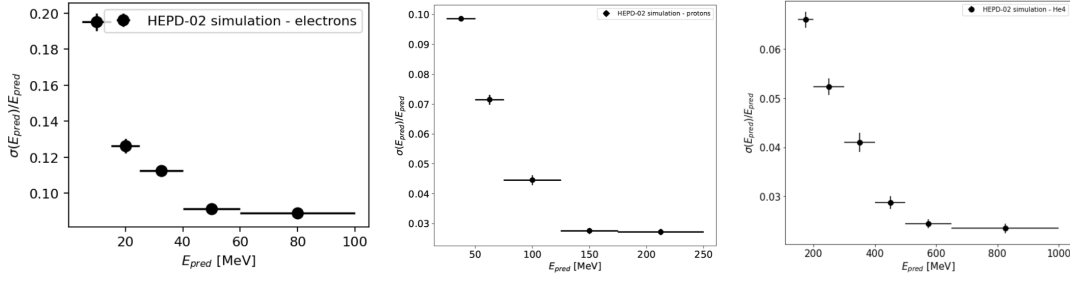


Figure 3: Energy resolution for electrons, protons and alpha particles as a function of the kinetic energy of the incoming particle.

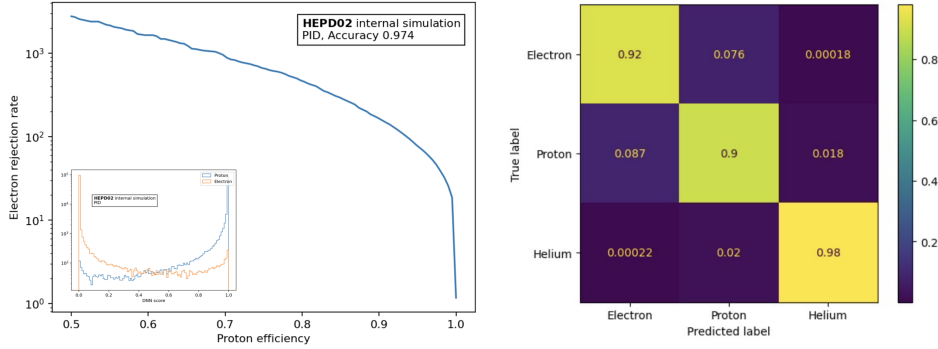


Figure 4: Receiver Operating Characteristic (ROC) curve for electron/proton discrimination (left) and the confusion matrix with the addition of helium nuclei as a third population are shown.

The reconstruction of the kinetic energy and of the particle identity is performed using a Deep Neural Network taking as input the calibrated signal coming from the PMTs connected to the scintillators, the cluster shapes and the track parameters (angles and residuals). This approach has the main advantage that correlations between variables are discovered and exploited automatically via the minimisation of the cost function. The Deep Learning-based reconstruction strategy exploits several information: (i) the correlations between PMTs responses; (ii) the positional information from TR1, TR2 and LYSO bars; (iii) the anti-correlation between polar angle and kinetic energy. The energy resolution on electrons, protons and helium nuclei is shown in figure 3. This approach automatically compensates for the energy lost in the passive components of the detector.

For what concerns the particle identification, another deep neural network exploiting the same information is trained to discriminate between electrons, protons and nuclei. The performance on simulated data can be seen in figure 4.

4. Preliminary results from test data

HEPD-02 performed an extensive calibration campaign with beam test sessions which ended at the beginning of July 2023. Moreover, several acquisitions of atmospheric muons were carried out in order to validate the detector response to minimum ionizing particles coming with an isotropic flux. These tests were necessary to study the performance of the different detector subsystems and

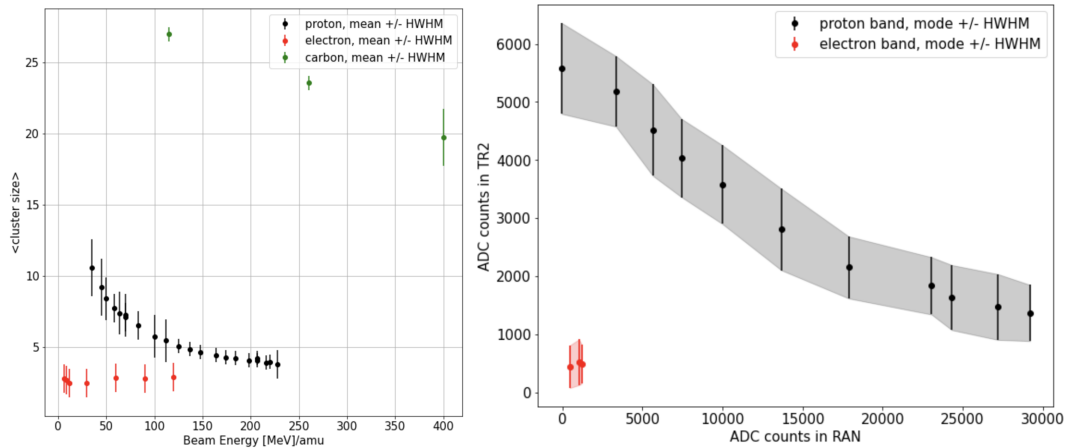


Figure 5: Particle identification strategy between different particles: cluster size vs energy (left) and TR2 ADC signal vs energy (right).

to validate its functionalities. The apparatus was tested in several facilities in Italy, with different particles and energies:

- photons and low energy electrons at 6, 9 and 12 MeV at the LINAC of Santa Chiara Hospital in Trento;
- protons in a wide range of energies from 30-200 MeV at the APSS Protontherapy center in Trento;
- high energy electrons from 30-120 MeV at the Beam Test Facility in Frascati;
- carbon nuclei from 115 MeV/amu to 398 MeV/amu at the CNAO in Pavia.

In these tests, one of the main focus was the discrimination of protons from low-energy electrons, which are the main target of the mission. In figure 5 two different discrimination strategies based on the tracker information (cluster size: number of close by pixel in a single cluster) and on the dE/dx approach using the TR2 bars signal vs the signal collected in the range calorimeter are shown.

The angular reconstruction capabilities have been validated with atmospheric muons and with vertical and inclined particle beams. Figure 6 shows the performance in the reconstruction of an isotropic flux and the pointing accuracy for a vertical 120 MeV electron beam. Very high pointing capability has been found and the angular resolution is compatible with the contribution coming from the irreducible Coulomb scattering.

The energy linearity of the EJ200 and LYSO calorimeter has been checked with dedicated runs with protons and carbon nuclei. The linearity of the High Gain ADC scale and of the Low Gain ADC scale can be seen from the plots beam energy vs ADC signal in figure 7.

5. Conclusions

The HEPD-02 detector will be launched in the early 2024 on board the CSES-02 satellite. It will measure fluxes of particles, such as electrons, protons and nuclei and it will have sensitivity

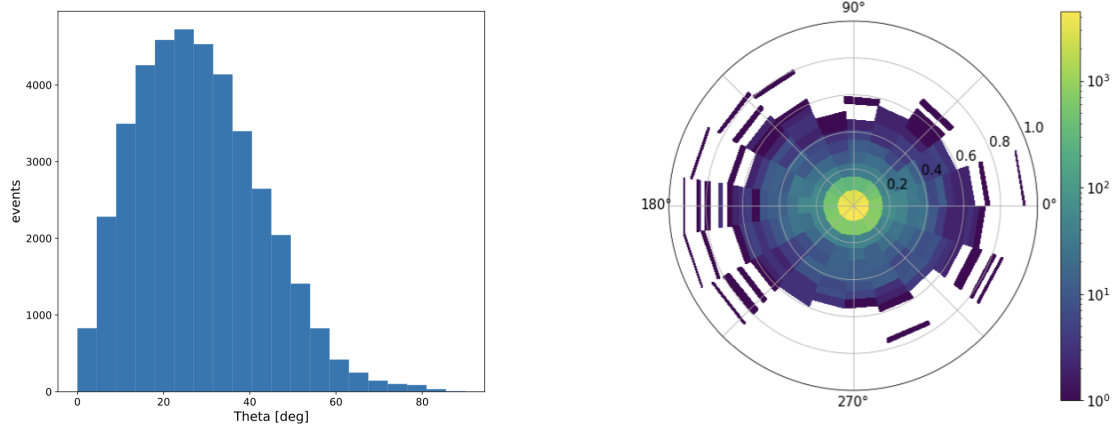


Figure 6: The polar angle reconstructed from an isotropic muon flux (left) and the pointing of a vertical beam of electrons in a plot $\sin \theta$ vs ϕ (right).

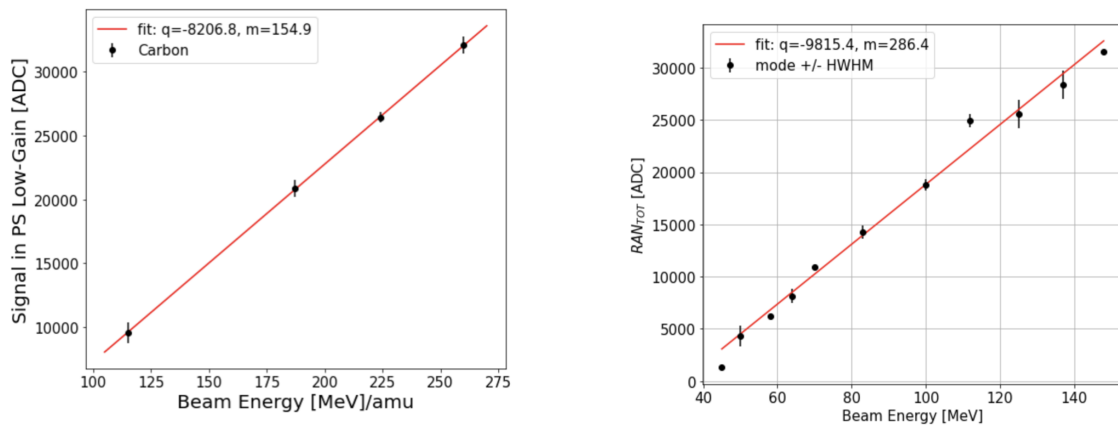


Figure 7: Energy linearity in the plastic scintillators in the LG scale with a carbon beam (left) and in the HG scale with a proton beam (right).

to Gamma Ray Burst. The addition of a second satellite will transform CSES in one of the few multi-satellite missions dedicated to cosmic rays. The increased coverage and the good geometric acceptance of HEPD-02 will improve the data gathering power of the mission. A detailed Monte Carlo (MC) simulation was developed and an extensive beam test campaign performed to validate HEPD-02 capabilities in identification and measurement of kinetic energy and arrival direction of incoming particles. In this contribution a synthetic description of the HEPD-02 detector and its main characteristics was given. The estimation of its scientific performances on MC simulation has been reported as well as preliminary performance on beam test acquisitions and atmospheric muon data.

References

- [1] P. Picozza et al. *The HEPD particle detector of the CSES satellite mission for investigating seismo-associated perturbations of the Van Allen belts*, J. Phys.: Conf. Ser. 798 012033 (2017)
- [2] M. Aguilar et al., *The Alpha Magnetic Spectrometer (AMS) on the international space station: Part II — Results from the first seven years*, Physics Reports Volume 894, Pages 1-116, 7 February (2021)
- [3] A. M. Galper et al. *The PAMELA experiment: a decade of Cosmic Ray Physics in space*, J. Phys.: Conf. Ser. 798 012033 (2017)
- [4] S. Bartocci et al. *Galactic Cosmic-Ray Hydrogen Spectra in the 40–250 MeV Range Measured by the High-energy Particle Detector (HEPD) on board the CSES-01 Satellite between 2018 and 2020*, The Astrophysical Journal, Volume 901, Number 1 (2020)
- [5] M. Martucci et al. *Time Dependence of 50–250 MeV Galactic Cosmic-Ray Protons between Solar Cycles 24 and 25, Measured by the High-energy Particle Detector on board the CSES-01 Satellite*, The Astrophysical Journal Letters, Volume 945, Number 2 (2023)
- [6] F. Palma et al. *The August 2018 Geomagnetic Storm Observed by the High-Energy Particle Detector on Board the CSES-01 Satellite*, Appl. Sci. 2021, 11(12), 5680
- [7] S. Agostinelli et al., *Geant4 simulation toolkit*, Nuclear Instruments and Methods in Physics Research A 506 250 (2003)
- [8] J. B. Birks, *Scintillations from Organic Crystals: Specific Fluorescence and Relative Response to Different Radiations*, Proceedings of the Physical Society. Section A, Volume 64, Number 10 (1951)
- [9] A. Di Luca et al., *TROPIX: A fast parametric tool reproducing the output of pixel detectors*, Proceedings of Science Pixel2022 (2023)
- [10] M. Ester, *A density-based algorithm for discovering clusters in large spatial databases with noise*, Proceedings of the Second International Conference on Knowledge Discovery and Data Mining, pp. 226–231 (1996)
- [11] P.V.C. Hough, *Methods and means for recognizing complex patterns*. US patent 3069654 (1962)

Full Authors List: Limadou HEPD Collaboration

R. Ammendola¹, D. Badoni¹, S. Bartocci¹, R. Battiston^{2,3}, S. Beolè^{4,5}, I. Bertello¹⁶, W.J. Burger^{3,6}, D. Campana⁷, G. Castellini⁸, P. Cipollone¹, S. Coli⁴, L. Conti^{1,9}, A. Contin^{10,11}, M. Cristoforetti^{12,3}, G. D'Angelo¹⁶, C. De Donato¹, C. De Santis¹, A. Di Luca^{12,3}, F.M. Follega^{2,3}, G. Gebbia^{2,3}, R. Iuppa^{2,3}, A. Lega^{12,3}, M. Lolli¹¹, M. Martucci^{1,13}, G. Masciantonio¹, M. Mergè^{18,1}, M. Mese^{7,14}, C. Neubuser³, F. Nozzoli³, A. Oliva¹¹, G. Osteria⁷, F. Palma¹, F. Palmonari^{10,11}, A. Parmentier¹⁶, B. Panico^{7,14}, S. Perciballi^{4,5}, F. Perfetto⁷, A. Perinelli^{2,3}, P. Picozza^{1,13}, M. Pozzato¹¹, G.M. Rebustini^{1,13}, E. Ricci^{2,3}, M. Ricci¹⁷, S.B. Ricciarini⁸, Z. Sahnoun^{10,11}, U. Savino⁵, V. Scotti^{7,14}, A. Sotgiu¹, R. Sparvoli^{1,13}, P. Ubertini¹⁶, V. Vilona³, V. Vitale¹, S. Zoffoli¹⁸ and P. Zuccon^{2,3}

¹ INFN-Sezione di Roma "Tor Vergata", V. della Ricerca Scientifica 1, I-00133 Rome, Italy;

² University of Trento, V. Sommarive 14, I-38123 Povo (Trento), Italy;

³ INFN-TIFPA, V. Sommarive 14, I-38123 Povo (Trento), Italy;

⁴ INFN-Sezione di Torino, Via P. Giuria 1, I-10125 Torino, Italy;

⁵ University of Torino, Via P. Giuria 1, I-10125 Torino, Italy;

⁶ Centro Fermi, V. Panisperna 89a, I-00184 Rome, Italy;

⁷ INFN-Sezione di Napoli, V. Cintia, I-80126 Naples, Italy;

⁸ IFAC-CNR, V. Madonna del Piano 10, I-50019 Sesto Fiorentino (Florence), Italy;

⁹ Uninettuno University, C.so V. Emanuele II 39, I-00186 Rome, Italy;

¹⁰ University of Bologna, V.le C. Berti Pichat 6/2, I-40127 Bologna, Italy;

¹¹ INFN-Sezione di Bologna, V.le C. Berti Pichat 6/2, I-40127 Bologna, Italy;

¹² Fondazione Bruno Kessler, V. Sommarive 18, I-38123 Povo (Trento), Italy;

¹³ University of Rome "Tor Vergata", V. della Ricerca Scientifica 1, I-00133 Rome, Italy;

¹⁴ University of Naples "Federico II", V. Cintia 21, I-80126 Naples, Italy;

¹⁵ INFN-Sezione di Firenze, V. Sansone 1, I-50019 Sesto Fiorentino (Florence), Italy;

¹⁶ INAF-IAPS, V. Fosso del Cavaliere 100, I-00133 Rome, Italy;

¹⁷ INFN-LNF, V. E. Fermi 54, I-00044 Frascati (Rome), Italy;

¹⁸ Italian Space Agency, V. del Politecnico, I-00133 Rome, Italy;